Supplementary Materials

Yu Luo, J. B. Pendry, and Alexandre Aubry

The Blackett Laboratory, Department of Physics, Imperial College London, London SW7 2AZ, UK

1. Dispersion of the surface plasmon excitation

Method to solve the periodic metallo-dielectric structures

Consider the problem of periodic slabs shown in Fig. 1.1. Suppose each element of the dipole array is located at ($x_k = 0$, $y_k = kd$, where $k = 0, \pm 1, \pm 2, \pm 3, \ldots$) as shown in Fig. 1.1. The potential generated by each element of the dipole array can be expanded by Fourier transformation in x direction.

$$-\phi = \frac{\overline{p} \cdot \overline{r}}{2\pi\varepsilon_0 r^2}\cos\omega t = \frac{1}{2\pi\varepsilon_0}\frac{xp_x + yp_y}{x^2 + y^2}\cos\omega t = \frac{1}{2\pi}\mathrm{Re}\left[\int dk a(k) e^{ikx - i\omega t}\right] \tag{1.1}$$

We find $a(k)$ by making a Fourier transform in the $y = constant$ plane. When $y > 0$

$$\begin{aligned} a(k) &= \frac{1}{2\pi\varepsilon_0}\int_{-\infty}^{\infty}\frac{xp_x + yp_y}{x^2 + y^2}e^{-ikx}dx = \frac{1}{2\pi\varepsilon_0}\int_{-\infty}^{\infty}\frac{xp_x + yp_y}{(x+iy)(x-iy)}e^{-ikx}dx \\ &= -2\pi i\,\mathrm{sgn}(k)\frac{1}{2\pi\varepsilon_0}\frac{-iyp_x\,\mathrm{sgn}(k) + yp_y}{-2iy\,\mathrm{sgn}(k)}e^{-|k|y} = \frac{p_y - ip_x\,\mathrm{sgn}(k)}{2\varepsilon_0}e^{-|k|y} = a_+ e^{-|k|y} \end{aligned} \tag{1.2}$$

Reworking the results for $y < 0$ gives

$$a(k) = \frac{-p_y - ip_x\,\mathrm{sgn}(k)}{2\varepsilon_0}e^{|k|y} = a_- e^{|k|y} \tag{1.3}$$

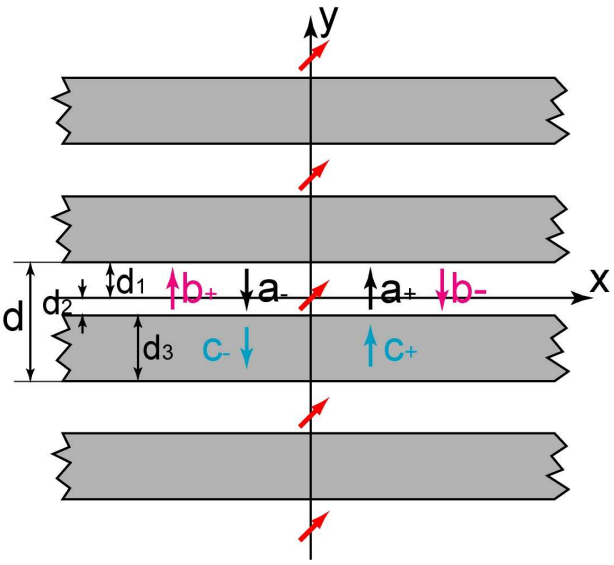

Fig. 1.1 Electrostatic potential induced by a dipole array embedded in periodic metallic slabs

Since the structure shown in Fig. 1.1 is completely periodic in y direction, solving the potential in one period will give the solution to the whole space. Here, we write the potential in each region of the period $-(d_2+d_3)<y<d_1$ as follow:

$$a_+e^{ikx-|k|y}+b_+e^{ikx-|k|y}+b_-e^{ikx+|k|y},\ \ 0<y<d_1 \tag{1.4}$$

$$a_-e^{ikx+|k|y}+b_-e^{ikx+|k|y}+b_+e^{ikx-|k|y},\ \ -d_2<y<0 \tag{1.5}$$

$$c_-e^{ikx+|k|y}+c_+e^{ikx-|k|y},\ \ -(d_2+d_3)<y<-d_2 \tag{1.6}$$

where b_- and b_+ are the expansion coefficients associated with the scattering potential, while c_-, and c_+ are the ones corresponding to the potential inside the metal. This four unknown coefficients can be determined by considering the normal boundary conditions and periodic boundary conditions:

$$(a_-+b_-)e^{-|k|d_2}+b_+e^{|k|d_2}=c_-e^{-|k|d_2}+c_+e^{|k|d_2} \tag{1.7}$$

$$(a_++b_+)e^{-|k|d_1}+b_-e^{|k|d_1}=c_-e^{-|k|(d_2+d_3)}+c_+e^{|k|(d_2+d_3)} \tag{1.8}$$

$$(a_-+b_-)e^{-|k|d_2}-b_+e^{|k|d_2}=\varepsilon c_-e^{-|k|d_2}-\varepsilon c_+e^{|k|d_2} \tag{1.9}$$

$$(a_++b_+)e^{-|k|d_1}-b_-e^{|k|d_1}=-\varepsilon c_-e^{-|k|(d_2+d_3)}+\varepsilon c_+e^{|k|(d_2+d_3)} \tag{1.10}$$

Solving Eq. (1.7)-Eq.(1.10) gives:

$$b_-=\frac{a_+e^{2|k|d_2+\alpha}\left(e^{2|k|d_3}-1\right)+a_-\left(1-e^{|k|(d_1+d_2+d_3)}\right)+a_-e^{2\alpha}\left(e^{|k|(d_1+d_2+d_3)}-e^{2|k|d_3}\right)}{e^{2\alpha}\left(e^{|k|(d_1+d_2)}-e^{|k|d_3}\right)^2-\left(e^{|k|(d_1+d_2+d_3)}-1\right)^2} \tag{1.11}$$

$$b_+=\frac{a_+\left(1-e^{|k|(d_1+d_2+d_3)}\right)+a_+e^{2\alpha}\left(e^{|k|(d_1+d_2+d_3)}-e^{2|k|d_3}\right)+a_-e^{2|k|d_1+\alpha}\left(e^{2|k|d_3}-1\right)}{e^{2\alpha}\left(e^{|k|(d_1+d_2)}-e^{|k|d_3}\right)^2-\left(e^{|k|(d_1+d_2+d_3)}-1\right)^2} \tag{1.12}$$

$$c_-=\frac{2e^{|k|(d_1+d_2+d_3)}}{\varepsilon+1}\frac{a_-\left(1-e^{|k|(d_1+d_2+d_3)}\right)+a_+e^{\alpha}\left(e^{|k|(-d_1+d_2+d_3)}-e^{2|k|d_2}\right)}{e^{2\alpha}\left(e^{|k|(d_1+d_2)}-e^{|k|d_3}\right)^2-\left(e^{|k|(d_1+d_2+d_3)}-1\right)^2} \tag{1.13}$$

$$c_+ = \frac{2}{\varepsilon+1}\frac{a_+\left(1-e^{|k|(d_1+d_2+d_3)}\right)+a_-e^{\alpha}\left(e^{|k|(d_1-d_2+d_3)}-e^{2|k|d_1}\right)}{e^{2\alpha}\left(e^{|k|(d_1+d_2)}-e^{|k|d_3}\right)^2-\left(e^{|k|(d_1+d_2+d_3)}-1\right)^2} \tag{1.14}$$

where $\alpha = \ln\left[(\varepsilon-1)/(\varepsilon+1)\right]$.

Cutoff feature of the structures

The dispersion of the surface plasmon excitation can be found through the condition that b_- and b_+ diverge,

$$e^{2\alpha}\left(e^{|k_p|(d_1+d_2)}-e^{|k_p|d_3}\right)^2-\left(e^{|k_p|(d_1+d_2+d_3)}-1\right)^2=0, \tag{1.15}$$

Eq. (1.15) gives two branches of surface plasmon excitations. We first consider the even mode where $\varepsilon<-1$. Substituting θ [where $\theta = 2\pi d_3/d$ when $d_1+d_2>d_3$; $\theta = 2\pi(d_1+d_2)/d$ when $d_1+d_2<d_3$] into Eq. (1.11), we obtain:

$$e^{\alpha}\sinh\left[\frac{|k_p|d}{2}\left(1-\frac{\theta}{\pi}\right)\right]=\sinh\left[\frac{|k_p|d}{2}\right] \tag{1.16}$$

Taking the limit $|k_p|\to 0$ in Eq. (1.15) yields

$$e^{-\alpha}=\left(1-\frac{\theta}{\pi}\right) \quad \text{or} \quad \varepsilon(\omega_c)=\frac{\theta-2\pi}{\theta} \tag{1.17}$$

This is the cutoff condition for the even mode, and ω_c is the lower bound cutoff frequency.

Similarly, for the odd mode of surface plasmon excitations, we can rewrite Eq. (1.15):

$$-e^{\alpha}\sinh\left[\frac{|k_p|d}{2}\left(1-\frac{\theta}{\pi}\right)\right]=\sinh\left[\frac{|k_p|d}{2}\right] \tag{1.18}$$

Taking the limit $|k|\to 0$, the cutoff condition for odd mode can be obtained:

$$-e^{-\alpha}=\left(1-\frac{\theta}{\pi}\right) \quad \text{or} \quad \varepsilon(\omega_c')=\frac{\theta}{\theta-2\pi} \tag{1.19}$$

where ω_c' is the upper bound cutoff frequency. We see from the above analysis that the surface plasmon excitations supported by the structure has two branches, namely the even branch which spans the frequency range $\omega_c < \omega < \omega_{sp}$ and the odd branch which spans the frequency range $\omega_{sp} < \omega < \omega_c'$. Here, ω_{sp} denotes the surface plasmon frequency where $\varepsilon\left(\omega_{sp}\right) = -1$

First order approximation of the surface plasmon wave number $\left|k_p\right|$

In order to further analyze the plasmonic properties of the structure, we need to calculate the surface plasmon wave number $\left|k_p\right|$. This can be achieved by applying a recurrence method to (1.15). Here, we also aim to find an approximate form of $\left|k_p\right|$.

Take the even mode as the example. When $\left|k_p\right| d \ll 1$, Eq. (1.16) is equivalent to

$$e^{\alpha} e^{(1-\theta/\pi)\left|k_p\right| d/2} = e^{\left|k_p\right| d/2}. \tag{1.20}$$

One can easily obtain:

$$\left|k_p\right| d = \frac{2\pi\alpha}{\theta} \tag{1.21}$$

This is the large scale approximation of $\left|k_p\right|$. Then in small scale limit $\left|k_p\right| d \ll 1$, we can expand the $\sinh$ function on both sides of Eq. (1.16), which yields

$$\left|k_p\right| d = 2\sqrt{6}\sqrt{\frac{1-\left(1-\theta/\pi\right)e^{\alpha}}{\left(1-\theta/\pi\right)^3 e^{\alpha} - 1}} \tag{1.22}$$

In Fig. 1.2 we plot the exact solution to $\left|k_p\right| d$ (red solid line) as well as the large scale approximation (black dashed line) and small scale approximation (blue dash-dot line) of $\left|k_p\right| d$ using Eq. (1.21) and (1.22). Interestingly, it appears that below the intersection point of the black dashed line and the blue dash-dot line, the small scale approximation curve (blue dash-dot line) nearly overlaps with the exact solution curve

(red solid line), while above this intersection point, the large scale approximation curve (black dashed line) agrees quite well with the exact solution curve (red solid line). This fact indicates that by appropriately connecting the small scale approximation with the large scale approximation, an accurate closed form of $|k_p|d$ can be obtained. Here, we write the approximate form of $|k_p|d$ in terms of the following segmented function:

$$|k_p|d = \begin{cases} \dfrac{2\pi\alpha}{\theta}, & \text{when } e^{\alpha} > \dfrac{1}{(1-\theta/\pi)^3} \text{ or } \sqrt{6}\sqrt{\dfrac{1-(1-\theta/\pi)e^{\alpha}}{(1-\theta/\pi)^3 e^{\alpha}-1}} > \dfrac{\pi\alpha}{\theta} \\ 2\sqrt{6}\sqrt{\dfrac{1-(1-\theta/\pi)e^{\alpha}}{(1-\theta/\pi)^3 e^{\alpha}-1}}, & \text{in all the other cases.} \end{cases} \tag{1.23}$$

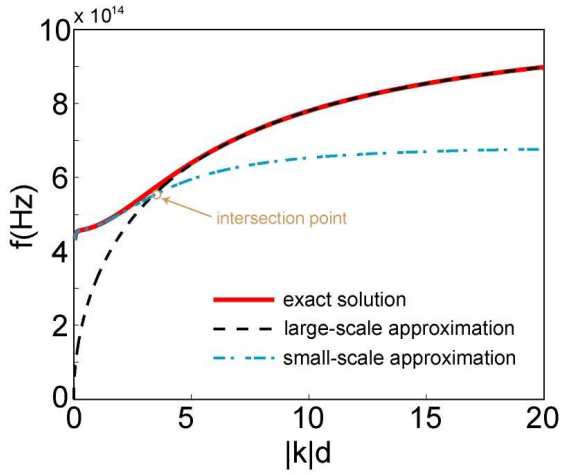

Fig. 1.2 Schematic of $|k_p|d$: The red solid line represents the exact solution to Eq. (1.15), while the black dashed line and blue dash-dot line correspond to the large scale limit and small scale limit of $|k_p|d$ using Eq. (1.20) and (1.21), respectively. Here we select the geometry parameters such that $d_3/d = 0.05$.

In Fig. 1.3, we plot the approximate solution of $|k_p|d$ given by Eq. (1.23) under three different cases. It is clear that the approximate form agrees quite well with the exact solution, demonstrating the validity of Eq. (1.23).

Similarly for the odd mode, detailed calculations show that the approximate form

of $|k_p|d$ can be written in terms of the following segmented function:

$$|k_p|d = \begin{cases} \dfrac{2\pi\alpha'}{\theta}, & \text{when } e^{\alpha'} > \dfrac{1}{(1-\theta/\pi)^3} \text{ or } \sqrt{6}\sqrt{\dfrac{1-(1-\theta/\pi)e^{\alpha'}}{(1-\theta/\pi)^3 e^{\alpha'}-1}} > \dfrac{\pi\alpha'}{\theta} \\ 2\sqrt{6}\sqrt{\dfrac{1-(1-\theta/\pi)e^{\alpha'}}{(1-\theta/\pi)^3 e^{\alpha'}-1}}, & \text{in all the other cases.} \end{cases} \tag{1.24}$$

where $\alpha' = \ln\left[(1-\varepsilon)/(\varepsilon+1)\right]$

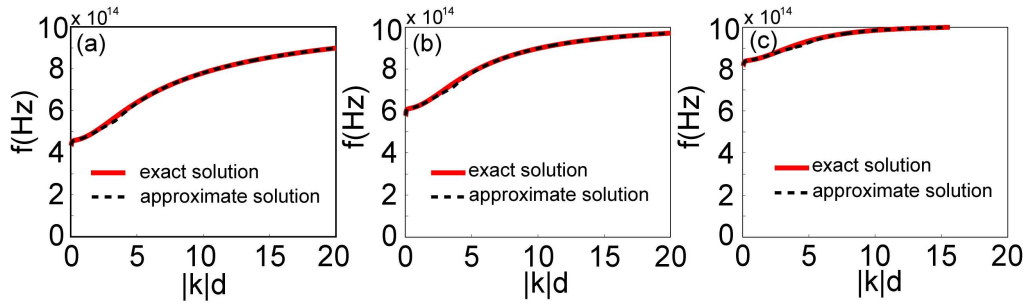

Fig. 1.3 Comparison of the exact solution to $|k_p|d$ (red solid line) and the approximate form (black dashed line) given by Eq.(1.22) under three different conditions: (a) $d_3/d = 0.05$; (b) $d_3/d = 0.1$; (c) $d_3/d = 0.25$.

2. Calculation of the field distribution, total power and total Raman signal in a volume

Potentials in the periodic slab geometry

Since we have already obtained the scattering coefficients b_- and b_+ in Sec. 1, the scattered potential in the region $0 < y < d_1$ can be determined by applying an inversed Fourier transform to Eq. (1.4) and (1.5). We have

$$-\phi_B = \frac{1}{4\varepsilon_0 d}\mathrm{Re}\left\{\left[\left(i\Gamma_y p_y + \mathrm{sgn}(x)\Gamma_x p_x\right)e^{k_p y} + \left(i\Lambda_y p_y + \mathrm{sgn}(x)\Lambda_x p_x\right)e^{-k_p y}\right]e^{ik_p|x|}\right\} \tag{2.1}$$

where $$\Gamma_x = \frac{\left(e^{2k_p d_3}-1\right)e^{2k_p d_2+\alpha} - e^{2k_p d_3+2\alpha} + \left(e^{2\alpha}-1\right)e^{k_p d} + 1}{\left(e^{k_p d}-1\right)\left[\left(\dfrac{d_1+d_2}{d}e^{k_p(d_1+d_2)+\alpha} - \dfrac{d_3}{d}e^{k_p d_3+\alpha}\right)\mathrm{sgn}(d_1+d_2-d_3) - e^{k_p d}\right]}$$

$$\Gamma_y = \frac{\left(e^{2k_p d_3}-1\right)e^{2k_p d_2+\alpha}+e^{2k_p d_3+2\alpha}-\left(e^{2\alpha}-1\right)e^{k_p d}-1}{\left(e^{k_p d}-1\right)\left[\left(\frac{d_1+d_2}{d}e^{k_p(d_1+d_2)+\alpha}-\frac{d_3}{d}e^{k_p d_3+\alpha}\right)\mathrm{sgn}\left(d_1+d_2-d_3\right)-e^{k_p d}\right]}$$

$$\Lambda_x = \frac{\left(e^{2k_p d_3}-1\right)e^{2k_p d_1+\alpha}-e^{2k_p d_3+2\alpha}+\left(e^{2\alpha}-1\right)e^{k_p d}+1}{\left(e^{k_p d}-1\right)\left[\left(\frac{d_1+d_2}{d}e^{k_p(d_1+d_2)+\alpha}-\frac{d_3}{d}e^{k_p d_3+\alpha}\right)\mathrm{sgn}\left(d_1+d_2-d_3\right)-e^{k_p d}\right]}$$

$$\Lambda_y = -\frac{\left(e^{2k_p d_3}-1\right)e^{2k_p d_1+\alpha}+e^{2k_p d_3+2\alpha}-\left(e^{2\alpha}-1\right)e^{k_p d}-1}{\left(e^{k_p d}-1\right)\left[\left(\frac{d_1+d_2}{d}e^{k_p(d_1+d_2)+\alpha}-\frac{d_3}{d}e^{k_p d_3+\alpha}\right)\mathrm{sgn}\left(d_1+d_2-d_3\right)-e^{k_p d}\right]}$$

The time dependence $e^{i\omega t}$ is implicit. Similarly, the potential in the metallic slab region $-\left(d_2+d_3\right)<y<-d_2$ can be obtained by applying an inversed Fourier transform to Eq. (1.6)

$$-\phi_C = \frac{1}{2\varepsilon_0 d}\mathrm{Re}\left\{\left[\frac{i\Theta_y p_y+\mathrm{sgn}\left(x\right)\Theta_x p_x}{\left(\varepsilon+1\right)}e^{k_p y}+\frac{i\Omega_y p_y+\mathrm{sgn}\left(x\right)\Omega_x p_x}{\left(\varepsilon+1\right)}e^{-k_p y}\right]e^{ik_p|x|}\right\} \quad (2.2)$$

where $$\Theta_x = \frac{e^{k_p(-d_1+d_2+d_3)+\alpha}-e^{2k_p d_2+\alpha}-e^{k_p d}+1}{\left(e^{k_p d}-1\right)\left[\left(\frac{d_1+d_2}{d}e^{k_p(d_1+d_2)+\alpha}-\frac{d_3}{d}e^{k_p d_3+\alpha}\right)\mathrm{sgn}\left(d_1+d_2-d_3\right)-e^{k_p d}\right]}$$

$$\Theta_y = \frac{e^{k_p(-d_1+d_2+d_3)+\alpha}-e^{2k_p d_2+\alpha}+e^{k_p d}-1}{\left(e^{k_p d}-1\right)\left[\left(\frac{d_1+d_2}{d}e^{k_p(d_1+d_2)+\alpha}-\frac{d_3}{d}e^{k_p d_3+\alpha}\right)\mathrm{sgn}\left(d_1+d_2-d_3\right)-e^{k_p d}\right]}$$

$$\Omega_x = \frac{1-e^{k_p d}+e^{k_p(d_1-d_2+d_3)+\alpha}-e^{2k_p d_1+\alpha}}{\left(e^{k_p d}-1\right)\left[\left(\frac{d_1+d_2}{d}e^{k_p(d_1+d_2)+\alpha}-\frac{d_3}{d}e^{k_p d_3+\alpha}\right)\mathrm{sgn}\left(d_1+d_2-d_3\right)-e^{k_p d}\right]}$$

$$\Omega_y = \frac{1-e^{k_p d}-e^{k_p(d_1-d_2+d_3)+\alpha}+e^{2k_p d_1+\alpha}}{\left(e^{k_p d}-1\right)\left[\left(\frac{d_1+d_2}{d}e^{k_p(d_1+d_2)+\alpha}-\frac{d_3}{d}e^{k_p d_3+\alpha}\right)\mathrm{sgn}\left(d_1+d_2-d_3\right)-e^{k_p d}\right]}$$

Potentials and the electric field in the wedge/groove geometry

Since the electrostatic potential is preserved under the conformal transformation $\phi(x,y)=\phi'(x',y')$, one can obtained the potential in the transformed wedge/groove geometry by simply substituting $\rho'=ae^{2\pi x/d}$, $\varphi'=2\pi y/d$, and $\overline{p}'=(2\pi a/d)\overline{p}$ in to Eq. (2.1) and (2.2). We have

$$-\phi_B{}'(\rho',\varphi')=$$
$$\frac{1}{8\pi\varepsilon_0 a}\mathrm{Re}\left\{\left[\begin{array}{l}\left(i\Gamma_y p_y'+\mathrm{sgn}(\rho'-a)\Gamma_x p_x'\right)e^{f_{\alpha,\theta}\varphi'/\pi}+\\ \left(i\Lambda_y p_y'+\mathrm{sgn}(\rho'-a)\Lambda_x p_x'\right)e^{-f_{\alpha,\theta}\varphi'/\pi}\end{array}\right]\left(\frac{\rho'}{a}\right)^{if_{\alpha,\theta}\mathrm{sgn}(\rho'-a)/\pi}\right\} \tag{2.3}$$

$$-\phi_C'(\rho',\varphi')=$$
$$\frac{1}{4\pi\varepsilon_0 a}\mathrm{Re}\left\{\left[\begin{array}{l}\dfrac{i\Theta_y p_y'+\mathrm{sgn}(\rho'-a)\Theta_x p_x'}{(\varepsilon+1)}e^{f_{\alpha,\theta}\varphi'/\pi}+\\ \dfrac{i\Omega_y p_y'+\mathrm{sgn}(\rho'-a)\Omega_x p_x'}{(\varepsilon+1)}e^{-f_{\alpha,\theta}\varphi'/\pi}\end{array}\right]\left(\frac{\rho'}{a}\right)^{if_{\alpha,\theta}\mathrm{sgn}(\rho'-a)/\pi}\right\} \tag{2.4}$$

where $f_{\alpha,\theta}=k_p d/2$ is a complex number determined by the following equation:

$$e^{\alpha}\sinh\left[(1-\theta/\pi)f_{\alpha,\theta}\right]=\sinh f_{\alpha,\theta} \tag{2.5}$$

And the first order approximation of $f_{\alpha,\theta}$ is

$$f_{\alpha,\theta}=\begin{cases}\dfrac{\pi\alpha}{\theta}, & \text{when } e^{\alpha}>\dfrac{1}{(1-\theta/\pi)^3} \text{ or } \sqrt{6}\sqrt{\dfrac{1-(1-\theta/\pi)e^{\alpha}}{(1-\theta/\pi)^3 e^{\alpha}-1}}>\dfrac{\pi\alpha}{\theta}\\ \sqrt{6}\sqrt{\dfrac{1-(1-\theta/\pi)e^{\alpha}}{(1-\theta/\pi)^3 e^{\alpha}-1}}, & \text{in all the other cases.}\end{cases} \tag{2.6}$$

Then we can calculate the scattered field:

$$E_{\rho}^{\mathrm{scatt}\prime}=\frac{\partial\phi_B'}{\partial\rho'}=$$
$$\frac{1}{8\pi^2\varepsilon_0 a\rho'}\mathrm{Re}\left\{f_{\alpha,\theta}\left[\begin{array}{l}\left(i\Gamma_x p_x'-\mathrm{sgn}(\rho'-a)\Gamma_y p_y'\right)e^{f_{\alpha,\theta}\varphi'/\pi}\\ +\left(i\Lambda_x p_x'-\mathrm{sgn}(\rho'-a)\Lambda_y p_y'\right)e^{-f_{\alpha,\theta}\varphi'/\pi}\end{array}\right]\left(\frac{\rho'}{a}\right)^{if_{\alpha,\theta}\mathrm{sgn}(\rho'-a)/\pi}\right\} \tag{2.7}$$

$$E_{\varphi}^{\text{scatt}\prime} = \frac{\partial \phi_B'}{\rho' \partial \varphi'} =$$

$$\frac{1}{8\pi^2 \varepsilon_0 a \rho'} \operatorname{Re}\left\{ f_{\alpha,\theta} \begin{bmatrix} \left(i\Gamma_y p_y' + \operatorname{sgn}\left(\rho' - a\right) \Gamma_x p_x' \right) e^{f_{\alpha,\theta}\varphi'/\pi} \\ -\left(i\Lambda_y p_y' + \operatorname{sgn}\left(\rho' - a\right) \Lambda_x p_x' \right) e^{-f_{\alpha,\theta}\varphi'/\pi} \end{bmatrix} \left(\frac{\rho'}{a} \right)^{if_{\alpha,\theta}\operatorname{sgn}(\rho'-a)/\pi} \right\} \tag{2.8}$$

Finally, the total scattered field strength can be obtained:

$$\begin{aligned} \left| \bar{E}'^{\text{scatt}} \right| &= \sqrt{\left| E_{\rho}'^{\text{scatt}} \right|^2 + \left| E_{\varphi}'^{\text{scatt}} \right|^2} \\ &= \underbrace{\frac{f_{\alpha,\theta}}{8\pi^2 \varepsilon_0 a \rho'}}_{\text{Compression factor}} \times \underbrace{\left(\frac{\rho'}{a} \right)^{-\operatorname{Im}\{f_{\alpha,\theta}\}\operatorname{sgn}(\rho'-a)/\pi}}_{\text{Dissipation loss}} \times \sqrt{A e^{2\operatorname{Re}\{f_{\alpha,\theta}\}\varphi'/\pi} + B e^{-2\operatorname{Re}\{f_{\alpha,\theta}\}\varphi'/\pi}} \end{aligned} \tag{2.9}$$

where $A = \left| i\Gamma_x p_x' - \Gamma_y p_y' \right|^2 + \left| i\Gamma_y p_y' + \Gamma_x p_x' \right|^2$, $B = \left| i\Lambda_x p_x' - \Lambda_y p_y' \right|^2 + \left| i\Lambda_y p_y' + \Lambda_x p_x' \right|^2$.

The first factor in Eq. (2.9) is a result of compression of space, while the second factor represents a decrease of the electric field along the radial ρ direction due to the metallic losses. Hence, whether the electric field diverges or vanishes at the vertex of the structure depends on the value of the two factors. And the critical condition can be found as

$$\operatorname{Im}\left\{ f_{\alpha,\theta} \right\} = \pi \quad . \tag{2.10}$$

Using the approximate form of $f_{\alpha,\theta}$ Eq. (2.6), Eq. (2.10) can be simplified to

$$\operatorname{Im}\left\{ \alpha \right\} = \theta \tag{2.11}$$

where $\alpha = \ln\left[\left(\varepsilon - 1 \right) / \left(\varepsilon + 1 \right) \right]$. Here we refer to the frequency for which Eq. (2.10) and Eq. (2.11) are satisfied as the critical frequency ω_0. Below ω_0 $\operatorname{Im}\left\{ \alpha \right\} < \theta$) and the electric field diverges at the vertex of the structure, even if the metal is highly dissipative. In contrast, above ω_0, $\operatorname{Im}\left\{ \alpha \right\} > \theta$ and the electric field decreases and finally vanishes as surface plasmons propagate towards the vertex.

Total power and total Raman signal in a volume

Although the electric field diverges below the critical frequency ω_0, the total power is still conserved. This fact can be demonstrated by integrating the power density over the whole space:

$$\begin{aligned}
&\int_0^{+\infty} d\rho' \int_0^{2\pi} \rho' d\varphi' \left|E'(\rho',\varphi')\right|^2 = \int_0^{+\infty} d\rho' \int_{\theta+\beta-2\pi}^{\beta} \rho' d\varphi' \left|E'^{\text{scatt}}_{\text{total}}\right|^2 + \int_0^{+\infty} d\rho' \int_{\beta}^{\beta+\theta} \rho' d\varphi' \left|E'^{\text{slab}}_{\text{total}}\right|^2 \\
&= \frac{\left|f_{\alpha,\theta}\right|^2 \left(A e^{\frac{\beta-\gamma}{\pi}\text{Re}\{f_{\alpha,\theta}\}} + B e^{\frac{\gamma-\beta}{\pi}\text{Re}\{f_{\alpha,\theta}\}} \right) \sinh\left[\left(2-\frac{\theta}{\pi}\right)\text{Re}\{f_{\alpha,\theta}\}\right]}{8\varepsilon_0^2 \,\text{Re}\{f_{\alpha,\theta}\}} \times \int_0^{+\infty} dx e^{-4\text{Im}\{f_{\alpha,\theta}\}x} \\
&\propto \int_0^{+\infty} dx e^{-4\text{Im}\{f_{\alpha,\theta}\}x}
\end{aligned} \tag{2.12}$$

where $\gamma = 2\pi - \beta - \theta$.. Since $\text{Im}\{f_{\alpha,\theta}\} > 0$, the above equation indicates that the total power always converges to a finite value:

$$\begin{aligned}
&\int_0^{+\infty} d\rho' \int_0^{2\pi} \rho' d\varphi' \left|E'(\rho',\varphi')\right|^2 \\
&= \frac{\left|f_{\alpha,\theta}\right|^2 \left(A e^{\frac{\beta-\gamma}{\pi}\text{Re}\{f_{\alpha,\theta}\}} + B e^{\frac{\gamma-\beta}{\pi}\text{Re}\{f_{\alpha,\theta}\}} \right) \sinh\left[\left(2-\frac{\theta}{\pi}\right)\text{Re}\{f_{\alpha,\theta}\}\right]}{32\varepsilon_0^2 \,\text{Re}\{f_{\alpha,\theta}\}\,\text{Im}\{f_{\alpha,\theta}\}}
\end{aligned} \tag{2.13}$$

Next, we consider the total Raman signal over the whole space. To a first order approximation, the Raman signal is proportional to $\left|E'_{\text{total}}\right|^4$. we have

$$\begin{aligned}
&\int_0^{+\infty} d\rho' \int_0^{2\pi} \rho' d\varphi' \left|E'(\rho',\varphi')\right|^4 = \int_0^{+\infty} d\rho' \int_{\theta+\beta-2\pi}^{\beta} \rho' d\varphi' \left|E'^{\text{scatt}}_{\text{total}}\right|^4 + \int_0^{+\infty} d\rho' \int_{\beta}^{\beta+\theta} \rho' d\varphi' \left|E'^{\text{slab}}_{\text{total}}\right|^4 \\
&\propto \int_0^{+\infty} dx e^{4\left(\pi - 2\text{Im}\{f_{\alpha,\theta}\}\right)x}
\end{aligned} \tag{2.14}$$

From Eq. (2.14), we see that under the condition $\pi > 2\,\text{Im}\{f_{\alpha,\theta}\}$ or $\theta > 2\,\text{Im}\{\alpha\}$, the total Raman signal diverges.

3. Absorption cross-sections of open crescents and rough surfaces

Since the energy is conserved under transformations, the power absorbed by the rough surfaces or open-crescent nano-structures in the transformed coordinate system z'' is equivalent to the power dissipated by the dipole in the original geometry z. Hence, we have:

$$\begin{aligned} P_a'' = P_d &= -\bar{E}\left(x=0, y=0\right)\frac{\partial}{\partial t}\bar{p}\cos\omega t \\ &= \omega\sin\omega t\left[p_x E_x\left(x=0, y=0\right) + p_y E_y\left(x=0, y=0\right)\right] \end{aligned} \tag{3.1}$$

Averaging the absorbed power over a circle of time yields

$$\tilde{P}_a'' = \omega\,\mathrm{Re}\left[\frac{k_p\left(\Gamma_x + \Lambda_x\right)}{8\varepsilon_0 d}\right]p_x^2 + \omega\,\mathrm{Re}\left[\frac{k_p\left(\Gamma_y - \Lambda_y\right)}{8\varepsilon_0 d}\right]p_y^2 \tag{3.2}$$

For the incidence power flux, we have

$$\tilde{P}_{inc}'' = \frac{1}{2}c_0\varepsilon_0\left|\bar{E}_{inc}''\right|^2 = \frac{c_0 a^2}{2\varepsilon_0 d^2 g^4}\left(p_x^2 + p_y^2\right) \tag{3.3}$$

Therefore the absorption cross-section for the capture of radiation can then be obtained as:

$$\sigma_a^x = \frac{\tilde{P}_a''^x}{\tilde{P}_{inc}''^x} = \frac{\omega g^4}{4c_0 a^2}\mathrm{Re}\left[k_p d\left(\Gamma_x + \Lambda_x\right)\right], \tag{3.4}$$

$$\sigma_a^y = \frac{\tilde{P}_a''^y}{\tilde{P}_{inc}''^y} = \frac{\omega g^4}{4c_0 a^2}\mathrm{Re}\left[k_p d\left(\Gamma_y - \Lambda_y\right)\right]. \tag{3.5}$$

Since $R\sin\theta = g^2/\left(2a\right)$ and $f_{\alpha,\theta} = k_p d/2$. The Eq. (3.4) and (3.5) can be written in terms of R

$$\sigma_a^x = \frac{2\omega R^2\sin^2\theta}{c_0}\mathrm{Re}\left[f_{\alpha,\theta}\left(\Gamma_x + \Lambda_x\right)\right], \tag{3.7}$$

$$\sigma_a^y = \frac{2\omega R^2\sin^2\theta}{c_0}\mathrm{Re}\left[f_{\alpha,\theta}\left(\Gamma_y - \Lambda_y\right)\right]. \tag{3.8}$$